Journal of Molecular Liquids 269 (2018) 511–520

Contents lists available at ScienceDirect

Journal of Molecular Liquids

journal homepage: www.elsevier.com/locate/molliq

Molecular insight into binding behavior of polyphenol (rutin) with beta lactoglobulin: Spectroscopic, molecular docking and MD simulation studies

Nasser Abdulatif Al-Shabib [a,*], Javed Masood Khan [a,*], Ajamaluddin Malik [b], Mohammad A. Alsenaidy [c], Md Tabish Rehman [d], Mohamed F. AlAjmi [d], Abdulrahman M. Alsenaidy [b], Fohad Mabood Husain [a], Rizwan Hasan Khan [e]

[a] Department of Food Science and Nutrition, Faculty of Food and Agricultural Sciences, King Saud University, 2460, Riyadh 11451, Saudi Arabia
[b] Protein Research Chair, Department of Biochemistry, College of Science, King Saud University, Riyadh, Saudi Arabia
[c] Department of Pharmaceutics, College of Pharmacy, King Saud University, Saudi Arabia
[d] Department of Pharmacognosy, College of Pharmacy, King Saud University, Riyadh 11451, Saudi Arabia
[e] Molecular Biophysics and Biophysical Chemistry Group, Interdisciplinary Biotechnology Unit, Aligarh Muslim University, Aligarh 202002, India

ARTICLE INFO

Article history:
Received 3 March 2018
Received in revised form 4 June 2018
Accepted 31 July 2018
Available online 03 August 2018

Keywords:
Rutin
Flavonoid
Protein-ligand interaction
beta lactoglobulin
CD
Molecular docking

ABSTRACT

The interaction of natural polyphenolic compounds (rutin) with β-lactoglobulin (BLG) was carried out by using several optical spectroscopic (UV–visible spectroscopy, fluorescence quenching measurements, synchronous fluorescence, 3D fluorescence spectroscopy and far-UV CD measurements), molecular docking and molecular dynamics (MD) simulation methods. The fluorescence quenching results confirmed that fluorescence intensity of BLG is quenched by rutin and the quenching constant is increased with increase in temperature. The quenching mechanism between rutin-BLG was found to be dynamic in nature. The thermodynamic parameter particularly ΔH^0 and ΔS^0 obtained through fluorescence measurements clearly indicated that hydrophobic forces are majorly involved in the rutin-BLG interaction. The UV-absorption, synchronous and three-dimensional fluorescence results displayed that the micro-environment of BLG is changed due to rutin interaction. The secondary structure of BLG was found higher in the presence of rutin. Molecular docking results suggested that rutin binds strongly in the internal cavity of BLG at site 1 and superficially at site 2 through both hydrogen bonding and hydrophobic interactions. The binding affinity was found to be higher $5.47 \times 10^6\ M^{-1}$ for site 1 compared to site 2 ($2.86 \times 10^5\ M^{-1}$). The MD simulation suggested that rutin formed a stable complex with BLG at site 1.This study will explain interacting properties of rutin with carrier BLG proteins and open a new vista for the food industry.

1. Introduction

The last couple of years, natural food additives found much more attention in public and food manufactures. Usually, the public is selecting those foods which do not have any additives, but if foods are not available without additives, then they chose natural additive containing foods instead of synthetic additives [1]. The known natural food additives are having antioxidants, antimicrobial properties. Apart from antioxidants and antimicrobial activity, natural food additives are also used for colorings and sweeteners. The antioxidants are chiefly used in food and its products to overcome off-flavors by oxidation of fats and resume the peroxidation. The polyphenols are very interesting natural food additives found in the vegetables and have several biological applications like antioxidant, reduce cancer, osteoporosis, cataract, brain disease and cardiovascular dysfunctions [2]. The polyphenols are entered into human diet through various roots for example fruits, vegetables, grains, bark roots, stem, flowers, tea and wine [3]. Flavonoids are a large group of the polyphenolic compound, which is found in plant foods and beverages [4]. Flavonols and flavones are the majority of dispersed flavonoids found in plant foods and beverages [5]. Rutin (Fig. 1A) is a flavonol, composed of quercetin and rutinose and found in many plants particularly buckwheat plant [6]. Rutin is very useful phytochemicals because of its important biological activities for example, antioxidant, antidiabetic, hormone therapy and neuroprotective [7]. Rutin attenuates the ischemic neural apoptosis because it stops p53 expression and lipid peroxidation and simultaneously increase the level of endogenous antioxidant defense enzymes [8]. Rutin is also showing antibacterial and

Abbreviations: BLG, β-lactoglobulin; CD, Circular dichroism; Trp, Tryptophan; K_A, binding constant.

* Corresponding authors at: Department of Food Sciences, College of Food and Agricultural Sciences, King Saud University, Riyadh, Saudi Arabia.
E-mail addresses: nalshabib@ksu.edu.sa (N.A. Al-Shabib), javedjmk@gmail.com (J.M. Khan).

https://doi.org/10.1016/j.molliq.2018.07.122
0167-7322/

antifungal activity against strains *Escherichia coli* and *Candida gattii* [9,10]. Several other biological activity such as *Anti-arthritic*, *Anti-Alzheimer*, *Anti-diabetic*, *Anti-cancer and Anti-viral* activity was recorded in published reports [11]. Due to lots of beneficial effects of rutin, the utilization of rutin-rich foods and beverages are found much more interest. Recently, it has been reported that flavonoids can affect the protein-ligand interactions also [12]. Thus, protein-flavonoids interactions need more attention in clinics. The binding of rutins with proteins are weakly understood. The clinical applications of rutin are limited because of very poor solubility in water and also have low bioavilabilty due to the hydrophobic ring structure. It is known that BLG is served as a good transporter for the hydrophobic ligand. The interaction of rutin with bovine β-lactoglobulin (BLG) will be important. Bovine BLG belongs to lipocalins family proteins. The general property of lipocalin family proteins, they are functionally different, having weak sequence homology but have similar tertiary structure. Majority of lipocalins proteins are involved in transport of compounds which have a low solubility such as vitamins, steroids and metabolic products etc. [13]. BLG is having the ability to interact and transfer small hydrophobic ligands easily [14]. The BLG is a major bovine whey protein with numerous genetic variants particularly A and B phenotypes are abundantly found [15]. BLG made up of 162 amino acids with 18.4 kDa of molecular weight and form calyx of almost 8-standard antiparallel β-sheet. BLG is found in dimeric state at physiological pH and become monomer close to pH 2 and 3 due to strong electrostatic repulsion between both subunits [16]. Computationally, it was seen that several polyphenols (quercetin and quercitrin) are known to bound in the internal cavity of BLG. However rutin is bound to the entrance of the cavity because of large structural volume [17]. Till date, no one has done spectroscopic binding and highly advanced computational measurements of rutin and BLG at physiological pH.

In the current work, the binding of BLG with rutin was evaluated by using several spectroscopic techniques and powerful molecular docking studies. The spectroscopic techniques reveled the kind of interaction was taking place between rutin and BLG protein. The binding constant, binding mode (dynamic or static) and thermodynamic parameters can also be evaluated by spectroscopic techniques [18]. The spectroscopic results can also designate the binding forces are involved between rutin and BLG interaction [19]. The conformational change of BLG was detected by far-UV CD measurements and 3D fluorescence spectroscopy. The molecular docking will describe the actual site of rutin interaction and also revealed the name of amino acids are involved in the interaction. BLG is important protein not only to understand the molecular properties but can also be used as drug carriers to distinct biological sites. This study may be helpful to hypothesize how herbivores fight to free radical scavenging by investigating the binding effectiveness of rutin to BLG.

2. Materials and methods

2.1. Materials

Bovine BLG (lot#SLBP8394V) and rutin was procured from Sigma Chemicals Co. (St. Louis, MO, USA). All other reagents and materials were used of analytical grade.

2.2. Solution preparations

All experiments were performed in 20 mM Tris-HCl buffer, pH 7.4. BLG was dissolved in 20 mM Tris-HCl buffer, pH 7.4 and dialyzed overnight in the similar buffer. After dialysis, BLG was filtered through 0.22 μ Millipore syringe filter. A BLG stock solutions concentration was calculated spectrophotometrically by taking absorbance at 280 nm, and extinction coefficient was taken 17,600 M^{-1} cm^{-1}. The 30 mg of rutin was dissolved in 5 mL of ethanol and covered with a dark sheet to avoid exposure of sunlight.

2.3. UV-visible spectroscopic measurements

Absorption measurements were carried out at 25 °C by using Agilent Technologies Carry 60 double beam UV–visible spectrophotometer attached with Peltier temperature controlled program. A fixed concentration of BLG (27.0 μM) was taken in every sample while rutin concentrations was varied from 5.0, 10.0 and 15.0 μM. The appropriate blank of rutin was also scanned and subtracted from BLG-rutin scanned spectra.

2.4. Steady state fluorescence quenching measurements

The Agilent Technologies Carry Eclipse fluorescence spectrophotometer is used and the instrument was equipped with a temperature holder and the temperatures were maintained by a constant temperature water circulator. The fluorescence emission spectra of BLG were recorded in the range of 300–400 nm after excitation at 295 nm. The excitation and emission slit width was fixed 5 and 10 nm respectively. The BLG concentrations were fixed 2.0 μM in all the measurements while rutin concentrations were varied from 0.0–6.6 μM. The fluorescence quenching was recorded at three different temperatures, i.e., 298, 310 and 318 °F and emission maximum were captured at 332 nm. The reduction in fluorescence intensity at 332 nm was estimated according to the Stren-Volmer equation (Eq. (1)).

$$\frac{F_0}{F} = K_{SV}[Q] + 1 = K_q\tau_0[Q] + 1 \tag{1}$$

$$kq = \frac{Ksv}{\tau 0} \tag{2}$$

where F_0 and F are the fluorescence intensities in the absence and presence of rutin, and K_{SV} is the Stern–Volmer quenching constant. The K_q is stands for the bimolecular rate constant in the quenching reaction and τ_0 is denoted as the average integral fluorescence lifetime of a fluorophore particularly tryptophan which is ~10^{-9} s [20]. The binding constants and binding sites were analyzed by using Eq. (3).

$$\log\left(\frac{F_0}{F} - 1\right) = \log K_b + n\ \log[Q] \tag{3}$$

where K_b is designated as binding constant and n is denoted as the number of binding sites.

Additionally, the standard enthalpy and entropy change were estimated by utilizing Van't Hoff equation at three different temperatures, given in Eq. (4).

$$\ln K_b = -\Delta H^\circ/RT + \Delta S^\circ/R \tag{4}$$

and

$$\Delta G^\circ = \Delta H^\circ - T\,\Delta S^\circ \tag{5}$$

where K_b is denoted as binding constant, T is absolute temperature, ΔH° is the change in enthalpy. ΔG° is known as change in free energy, ΔS° is entropy change, R is gas constant (8.314 J/ mol K^{-1}).

The appropriate blank of rutin was taken in all the steady state fluorescence-quenching measurements.

2.5. Synchronous fluorescence

The synchronous fluorescence spectral measurements of rutin–BLG were taken at different scanning intervals of Δλ (Δλ = Δλex −Δλem). The spectral behavior of tyrosine and tryptophan amino acid residues of BLG was recorded at Δλ = 15 nm and Δλ = 60 nm, respectively. The spectra were scanned in the range of 200–500 nm. The concentration of BLG was fixed at 2.0 μM whereas the concentration

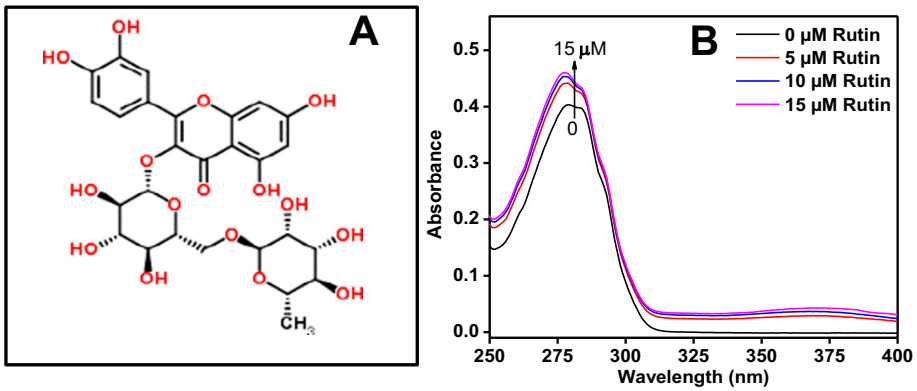

Fig. 1. Molecular structure of rutin (A). (B). Absorption spectra of BLG alone and gradually titrated with rutin at room temperature. BLG (27.0 μM) (—) and rutin (—) 5.0, (—) 10.0, and (—) 15.0 μM concentrations was used.

of rutin was varied from 0.33 μM to 6.5 μM. The excitation and emission slit width were kept constant 10.0 nm.

2.6. 3D fluorescence spectra

The 3D fluorescence spectra of BLG were monitored with and without rutin. The final concentrations of BLG and rutin taken were 2.0 μM respectively. The 3D fluorescence spectra of the sample with and without rutin was scanned by excitation wavelength in the range of 200–500 nm and emission wavelength from 200 to 600 nm at an interval of 5 nm. The scanning parameters were the same as in the fluorescence quenching experiments.

2.7. Far-UV CD measurements

The secondary structural modification of BLG in the absence and presence of rutin was examined by using Applied Photophysics, Chirascan Plus, UK spectropolarimeter attached with a Peltier-type temperature controller. Before sample measurements, the CD instruments were calibrated with D-10-camphorsulfonic acid. Each spectrum was

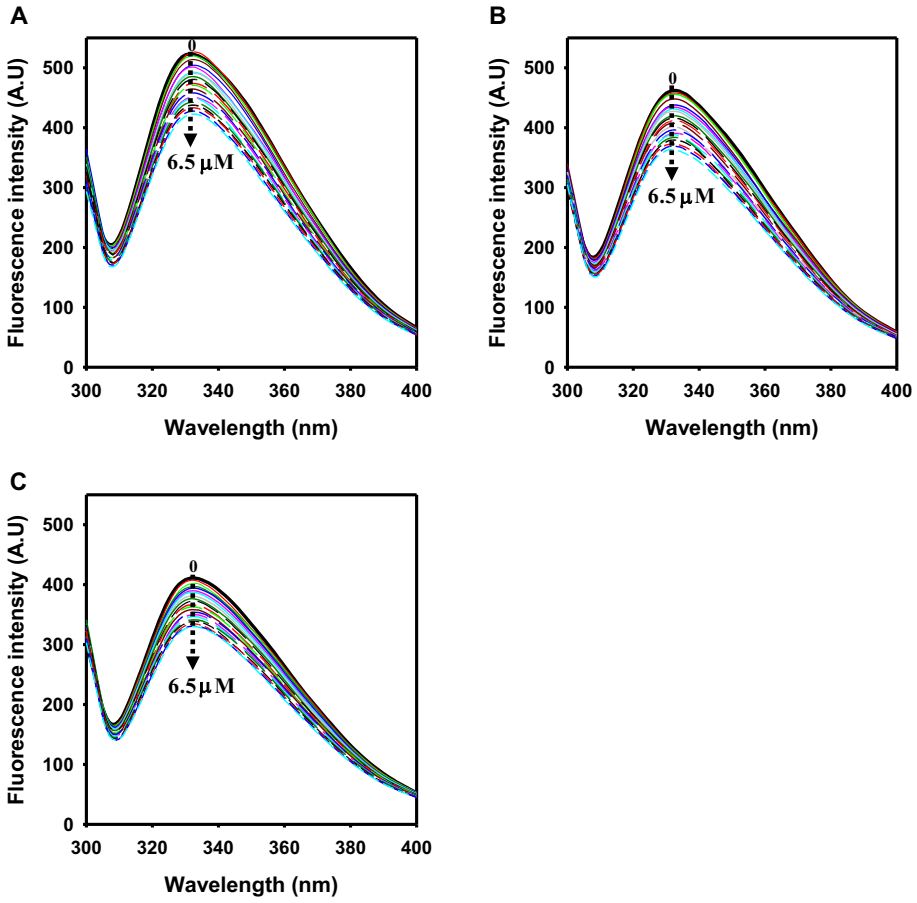

Fig. 2. Fluorescence emission spectra of BLG (2.0 μM) in the absence and presence of increasing concentrations of rutin (0.33 to 6.5 μM) at (A) 298 K, (B) 310 K and (C) 318 K. The sample was excitation at 295 nm and emission was recorded from 300 to 400 nm at physiological pH.

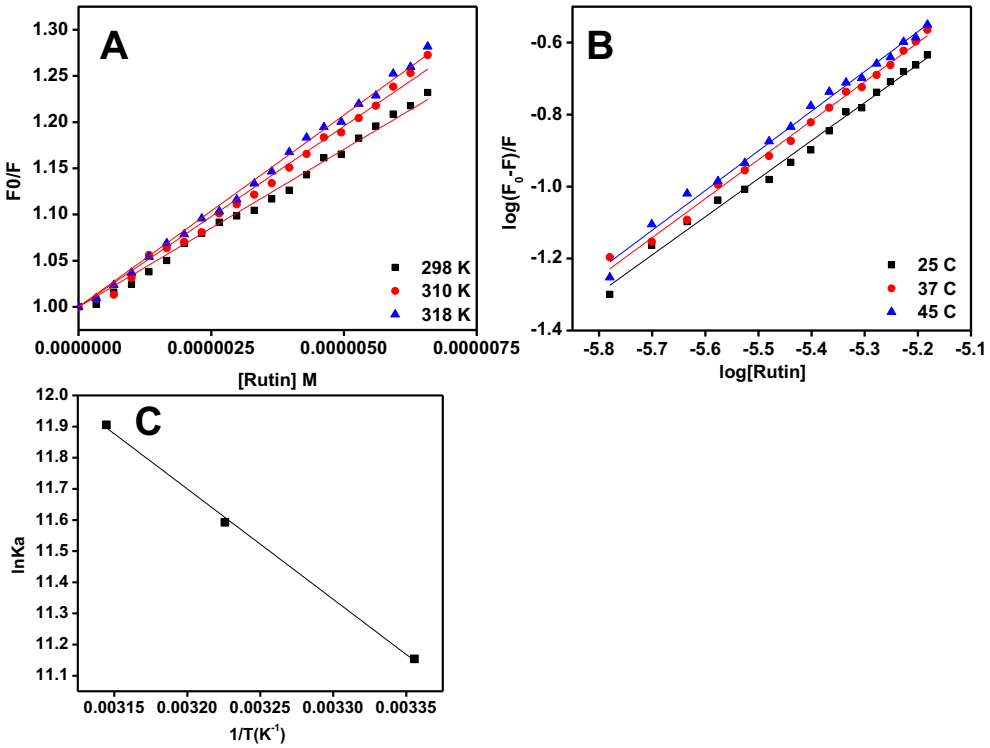

Fig. 3. The Stern–Volmer plots for the binding of rutin with BLG at 298 (-■-), 310 (-●-) and 318 (-▲-) K (A). (B) Plot between log [(F0/F)-1] and log [rutin] for BLG–rutin interaction at 298 (-■-), 310 (-●-) and 318 (-▲-) K. The sample was excitation at 295 nm and concentrations of BLG (2.0 μM) and Rutin (0–6.5 μM) was taken. (C) Van't Hoff plot for temperature dependence of Kb calculation. The data Obtained from BLG fluorescence quenching by rutin at 298, 310 and 318 K at physiological pH.

recorded on the average of three scans. The far-UV CD spectra of BLG were recorded in the range 200–250 nm. The obtained far-UV CD data were further converted into mean residue ellipticity (MRE) which is displayed in Eq. (7).

$$\mathrm{MRE} = \frac{\theta\mathrm{obs}\ (\mathrm{medg})}{10\ \mathrm{X}\ \mathrm{n}\ \mathrm{X}\ \mathrm{Cp}\ \mathrm{X}\ \mathrm{l}} \tag{6}$$

where θ_{obs} is the CD in millidegrees, n is the number of amino acid of BLG, and l is the path length of the cell in centimeters and Cp is the molar fraction of BLG. The percent secondary structure of BLG at different rutin concentrations was calculated by CDNN software.

2.8. Molecular docking and simulation study

MAESTRO (Maestro, Schrödinger, LLC, New York, NY, 2017) was used for all the steps involved in protein and ligand preparation, receptor grid generation and docking.

2.9. Proteins preparation

The X-ray crystal structure of BLG (PDB Id: 3NPO, resolved 2.20 Å) [21] was downloaded from PDB database (http://www.rcsb.org/pdb). Protein preparation wizard of GLIDE (Glide, Schrödinger, LLC, New York, NY, 2017) was used for the assessment and refinement of protein structure before performing molecular docking. The structure of the protein was prepared by removing water molecules, adding missing hydrogen atoms, assigning bond orders, creating zero bond order to disulfide bonds and deleting any other hetero atoms expect respective ligands. Missing loops and any side chains were added using PRIME module of Schrodinger software (Prime, Schrödinger, LLC, New York, NY, 2017). The protein was then optimized to create H-bond network, and finally energy was minimized using the optimized potentials for liquid simulations 2005 (OPLS2005) force field by setting a default constraint of 0.30 Å root-mean-square deviation (RMSD).

2.10. Ligand preparation

The structure of rutin was drawn using 2D sketcher of Schrodinger suite and optimized for docking by assigning the bond orders and angles using LigPrep module (LigPrep, Schrödinger, LLC, New York, NY, 2017). In LigPrep module, the 2D structure of rutin was converted into the 3D structure, and the energy was minimized using OPLS2005. The ionization state of rutin was generated at pH 7.0 ± 2.0 with the help of Epik module of LigPrep (Epik, Schrödinger, LLC, New York, NY, 2017), keeping other parameters to default values.

2.11. Grid generation and Molecular docking

The active site of BLG was predicted using SiteMap module of Schrodinger software (Sitemap, Schrödinger, LLC, New York, NY, 2017). The grid box was generated by selecting the centroid of the map as the centroid of the grid box. The grid size for docking has been decided by picking the centroid of the respective sites (Site 1 and Site 2) as the center of the grids. The grid size of site 1 was 80 × 80 × 80 Å, while for site 2 the grid size was 56 × 56 × 56 Å. Molecular docking of rutin with BLG was performed with the help of GLIDE v.6.7 from the Schrödinger Suite. Standard precision (SP) and extra precision (XP) docking calculations were carried out and the parameters of scaling

Table 1
The SterneVolmer quenching constants (KSV), bimolecular quenching rate constants (kq), number of binding sites (n) and binding constant (K_A) calculated in the BLG-rutin interaction at pH 7.4 at three different (298, 310 and 318) temperatures.

S. No.	T (K)	Ksv.10^{-4} (L/mol)	Kq.10^{-12} (L/mol/s)	R^2	n	K_A. 10^{-5} (L/mol)
1	298	3.4	3.4	0.9934	1.05	0.69
2	310	3.9	3.1	0.9929	1.08	1.08
4	318	4.1	4.1	0.9973	1.10	1.48

Table 2
The thermodynamic changes enthalpy change (ΔH), entropy change (ΔS) and Gibbs' free energy change (ΔG) values for binding of BLG:rutin at 298 K, 310 K and 318 K.

S. No.	T (K)	−ΔG (KJ/mol)	ΔH (KJ/mol)	ΔS (J/mol/K
1	298	−63.6428	29.57	191.57
2	310	−68.8078		
3	318	−72.4916		

factor and partial charge cutoff were set at the default values 0.80 and 0.15, respectively. MM-GBSA (Molecular Mechanics-General Born Surface Area) calculation was performed for the estimation of binding energy. Post docking analysis and visualization was performed on Maestro. The binding affinity of rutin with BLG was calculated as described earlier [22,23] using the following relation:

$$\Delta G = -RT \ \ln Kd \quad (7)$$

where, ΔG is the binding energy, T is temperature, R is Boltzman gas constant ($R = 1.987$ cal/mol/K) and Kd is the binding affinity.

2.12. Molecular dynamics (MD) simulation

Molecular dynamics simulation was performed using Desmond module of Schrodinger suite (Desmond, Schrödinger, LLC, New York, NY, 2017). The docked complex of rutin at site 1 of BLG was used as an initial conformation for performing MD simulation using OPLS2005 forcefield. Molecular system was placed in an orthorhombic box in such a way that a buffer region of 10 Å was maintained between protein atoms and boundaries of the box. TIP3P water molecules was used to solvate the system and it is neutralized by adding $25Na^+$ and $17Cl^-$ ions. The system was minimized and subjected to 30 ns MD simulation with NPT ensemble at 300 K temperature and 1.013 bar pressure while keeping other settings to their default values. In the MD simulation, a time step of 2 fs was used, while the energy and trajectory coordinates were recorded for every 5 ps. Maestro was used for analyzing trajectories and calculating RMSDs from initial structures.

3. Results and discussion

3.1. UV-visible absorption spectroscopy

The UV-absorption spectroscopy is utilized to get the information about secondary (far-UV) and tertiary (near-UV) structural change of proteins [24,25]. The chromophores of proteins particularly (tryptophan, tyrosine and phenylalanine) showed specific electronic absorption bands in between 255 and 300 nm. The aromatic amino acids particularly tryptophan displayed absorption peak exclusively around 280 nm [26]. UV-visible absorption measurements were made at pH 7.4, the maximal absorption wavelength of BLG was seen close to 280 nm. The native BLG protein and BLG complex with increasing concentrations of rutin (5.0, 10.0 and 15.0 μM) are shown in Fig. 1B. From the Fig. 1B, it can be seen that the peak intensity at 280 nm was found increased in the presence of increasing concentrations of rutin but the peak position was remain same at all rutin concentrations. The increase in absorption band at 280 nm in response to rutin is indicated that the BLG conformation is changed due to rutin binding and the changes are centered near tryptophan residues. Similar absorptions changes were also recorded in case of butylated hydroxytoluene-human serum albumin interaction [27].

3.2. The mechanism of fluorescence quenching in BLG-rutin interaction

The intrinsic fluorescence of proteins (BLG) comes from aromatic amino acids viz., tryptophan (Trp), tyrosine (Tyr) and phenylalanine (Phe). These amino acids are frequently targeted to investigate the ligands or drugs induced conformational changes in proteins [28]. Among above amino acids residues, Trp has highest fluorescence intensity and very sensitive to the changes in the microenvironment. BLG contains two Trp residues (Trp19 and Trp61), the Trp19 residues is present inside the core of BLG while Trp61 is present at the surface [29]. Trp19 is only suitable probe to check the binding between rutin and BLG protein as it is buried inside the cavity while Trp61 is exposed to the solvent. The fluorescent spectra of BLG alone and with different concentrations of rutin at three different temperatures (298, 310 and 318 °F) were recorded and the results are presented in Fig. 2A–C. From the figures, it was seen that BLG had a strong fluorescence emission at 332 nm after being excited at 295 nm and the fluorescence intensity was slightly decrease with respect to increase in temperature. The maximum fluorescence intensity was found at 298 ≥ 310 ≥ 318 °F. The fluorescent intensity of BLG was also decreases continuously with increase in rutin concentration, while the wavelength maximum was slightly blue shifted at all the temperatures. The change in fluorescence intensity and wavelength maximums are suggesting that a change was found around fluorophores and the rutin is interacting close to Trp residue of BLG. It is reported that the fluorescence intensity is decreased with increase in temperature because of quenching mechanism [30]. The fluorescence quenching mechanism of protein is divided into three way (i) static (ii) dynamic and (iii) both dynamic and static. In static quenching, a complex is formed between drugs and protein, in dynamic quenching-a collision was taking place between drugs and proteins and in case dynamic and static quenching-both collision and complex are formed together in the presence of drugs [31]. The dynamic and static quenching can be differentiated on the basis of temperature. In dynamic quenching, quenching constant increase with increase in temperature and vice versa in case of static quenching [32]. In order to investigate the quenching mechanism involved in rutin-BLG interaction, rutin was titrated with BLG at three different temperatures and

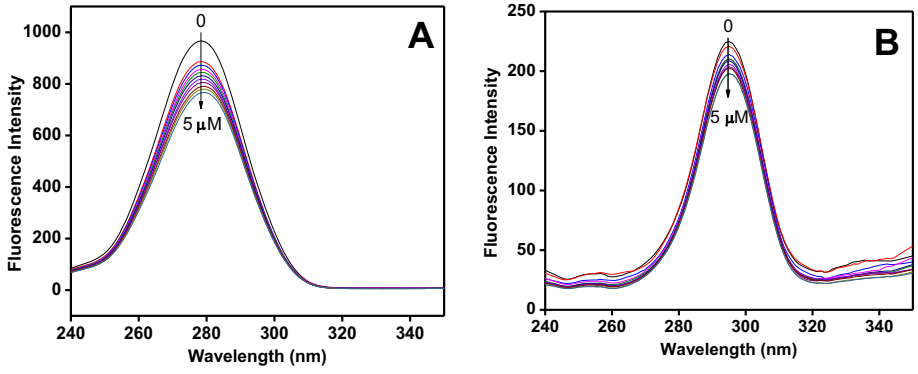

Fig. 4. Synchronous fluorescence spectrum of BLG. (A) Δλ = 60 nm, (B) Δλ = 15 nm. BLG concentrations was taken 2.0 μM, and rutin concentration was varied from 0.5 to 5.0 μM at pH 7.4.

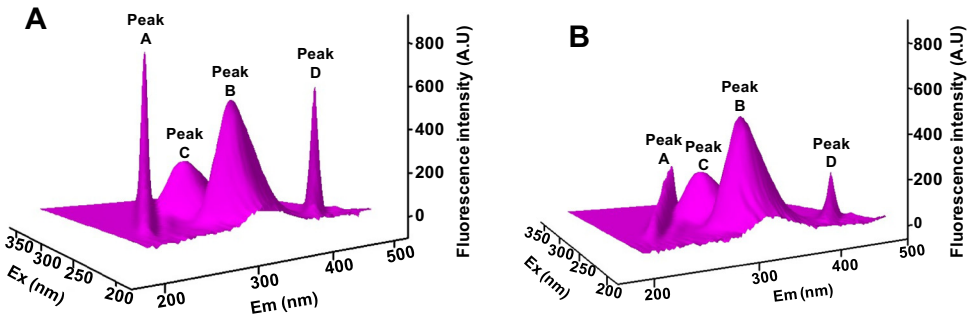

Fig. 5. Three-dimensional fluorescence spectra of BLG (A) and BLG-rutin (B). The concentration of BLG and rutin was taken 2.0 μM respectively.

the obtained results were examined according to the Stern–Volmer equation (as equation no 1). Fig. 3A shows Stern–Volmer plots for rutin-BLG system at three different temperatures viz. 298, 310 and 315 °F and the plot was found to be linear. The Stern–Volmer quenching constant (K_{SV}) values were determined from the slopes of these plots and the values are given in Table 1. From the Fig. 3A and Table 1, it is evident that the Ksv values at 298, 310 and 315 °F were found to be 3.4, 3.9 and 4.1 10^{-4} L/ mol respectively; the increase in Ksv values with temperature indicated that the dynamic quenching mechanism was found to take place between rutin-BLG. Similar quenching mechanism was also found in case of anastrozole-BSA interaction [33]. The obtained Ksv values help to calculate bimolecular quenching rate constant by using the following Eq. (2). The fluorescence lifetime of the biopolymer was found 10^{-8} s [34]. The values of bimolecular quenching constant are listed in Table 1. The values are increased with increased in temperature, which is also supporting the dynamic mode of quenching between rutin-BLG. The maximum scatter collision-quenching constant Kq of various quencher with other biomolecules are found around 2 × 10^{10} L/ mol s^{-1} [35]. Hence, the quenching rate constant of rutin-BLG is found more than quenching constant of biomolecules.

3.3. Binding constant and number of binding sites was determined in rutin-BLG interaction

The binding constant and number of binding sites was calculated by utilizing Eq. (3). The slope of Eq. 3 plot gives information about number of binding sites (n) and intercept provide binding constant (K_A) of the rutin-BLG interaction. The values of K_A and n are shown in Fig. 3B and Table 1. From the Table 1 and Fig. 3B, it was noticed that the values of binding constant increase with increase in temperature. The binding constant values are also supporting that the quenching between rutin and BLG was found dynamic type. The number of binding sites was found slightly >1, listed in Table 1.

Table 3
Three-dimensional fluorescence spectral parameters of BLG and BLG-rutin.

S.No.	Condition	Peak	Peak position (λex/λem, nm/nm)	Intensity
1	BLG alone	A	350/350	840.5
2		B	285/334	241.0
3		C	295/332	528.0
4		d	250/481	633.8
5	BLG+2.0 μM rutin	A	350/350	221.53
6		B	285/334	214.09
7		C	295/332	475.60
8		D	250/481	213.05

3.4. Determination of the binding forces between rutin-BLG interactions

The binding forces involved in rutin and BLG interaction can be calculated with the help of thermodynamic parameters. Usually, biomolecules can interact with ligand or drugs through four types of interaction namely (i) hydrophobic interaction, (ii) hydrogen bonding, (iii) Van der Waals' interaction and (iv) electrostatic interaction [36]. Ross and Subramanian have clearly stated that the thermodynamic laws are used to investigate the types of binding forces involved between ligand and biomolecules [37]. The values of enthalpy (ΔH) and entropy (ΔS) for rutin–BLG interaction were examined from the van't Hoff plot (Fig. 3C) by fitting the K_A values obtained at three different temperatures into Eq. (4), while the values of ΔG at these temperatures were calculated by using Eq. (5). The data of these thermodynamic parameters are listed in Table 2. The values of ΔG was found negative at all the temperature confirming that the rutin-BLG reaction is spontaneous. The values of ΔH and ΔS are found positive during rutin-BLG interaction; the positive values of enthalpy and entropy are suggesting that the reaction is endothermic. The positive sign of ΔH and ΔS are found when the ligand interacts with biomolecules through hydrophobic interaction [38]. The rutin-BLG thermodynamic parameters are suggesting that hydrophobic residues of BLG were involved in interaction with rutin.

3.5. Synchronous fluorescence spectroscopy

Synchronous fluorescence spectroscopy is applied to characterize the modification around microenvironment of fluorophores. Two very common fluorophores (tryptophan and tyrosine) were targeted to see

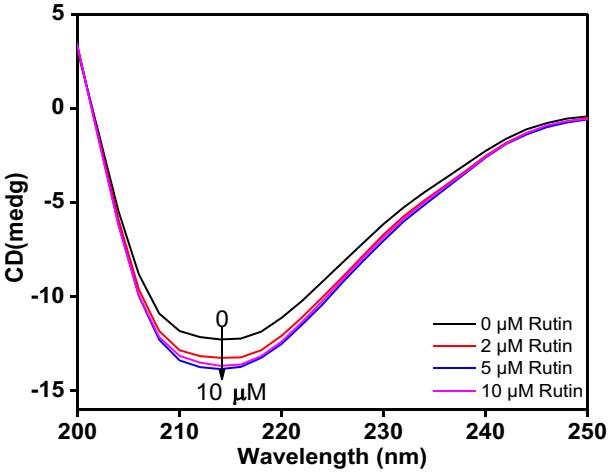

Fig. 6. Far-UV CD spectra of the Rutin-BLG system. The BLG concentrations was take 0.2 mg ml^{-1} and rutin concentration was varied 2.0 (—), 5.0 (—) and 10.0 (—) μM at temperature 298 K.

Table 4
Percent secondary structure content of BLG upon interaction with rutin.

S. No.	Conditions	% Helix	% Antiparallel	% Parallel	% Beta-turn	% Random coil
1	BLG alone	22.4	12.8	11.8	18.8	39.8
2	BLG + 2 μM rutin	20.0	14.0	13.2	19.8	40.5
3	BLG + 5 μM rutin	19.2	15.9	13.8	19.9	40.6
4	BLG + 10 μM rutin	18.6	16.0	14.10	19.9	40.8

the changes around microenvironment. If the Δλ values between excitation and emission wavelength are 15 and 60 nm, the synchronous fluorescence gives information around tyrosine and tryptophan residues respectively. The synchronous fluorescence spectra of BLG for Δλ 60 and 15 nm were plotted in the presence of rutin are shown in Fig. 4. The emission peak of both tryptophan and tyrosine residues is not shifted significantly with rutin concentration while fluorescence intensity is gradually decreased. The drop in fluorescence intensity was found more in case of tryptophan fluorescence. The synchronous fluorescence results signified that the conformational changes are chiefly occurred near tryptophan residues.

3.6. Three dimensional fluorescence spectroscopic analysis

Three-dimensional (3D) fluorescence spectroscopy is one of the powerful techniques, which can give comprehensive detailed fluorescence information of protein into more scientific and credible manner. 3D fluorescence spectroscopy is employed to investigate the rutin-induced conformational change of BLG protein. In Fig. 5, the native BLG showed four peaks, peak A is the Rayleigh scattering peak (λex = λem) and peak D is the second-order scattering peak (λem = 2λex) [39]. The values of all the peaks are shown in Table 3. The main peak of tryptophan and tyrosine residues is peak B while peak C is showed the fluorescence of protein backbone structure of π-π* (C=O) [40]. The scattering peak A and D was reduced in the presence of 2.0 μM of rutin and the reduction in scattering peak of BLG is suggesting that the rutin-BLG interacted each other. The fluorescence intensity of main peak B and C was also decreased in the presence of 2.0 μM of rutin. The decrements in fluorescence intensity of all four peaks are suggesting that the rutin is causing some conformational change in BLG protein. Similar conformational change around microenvironment was found when ranitidine (RTN) interacted with human serum albumin [41].

3.7. Far-UV Circular dichroism (CD)

Far-UV CD is very useful technique to examine the conformational changes of proteins at secondary structure level [42–44]. To investigate the possible changes in the secondary structure of BLG upon binding with rutin, far-UV CD experiments were done at room temperature. Far-UV CD spectra of free BLG and with different concentrations of rutin were shown in Fig. 6. It can be seen from the figure that the free BLG is showing a single negative peak at 218 nm in the far-UV region, which is characteristic of typical β-sheet structure of protein [45]. With increasing concentrations of rutin the negative ellipticity at 218 nm was increasing, the increase in negative ellipticity in response to rutin is indicating that the BLG is gaining more secondary structure.

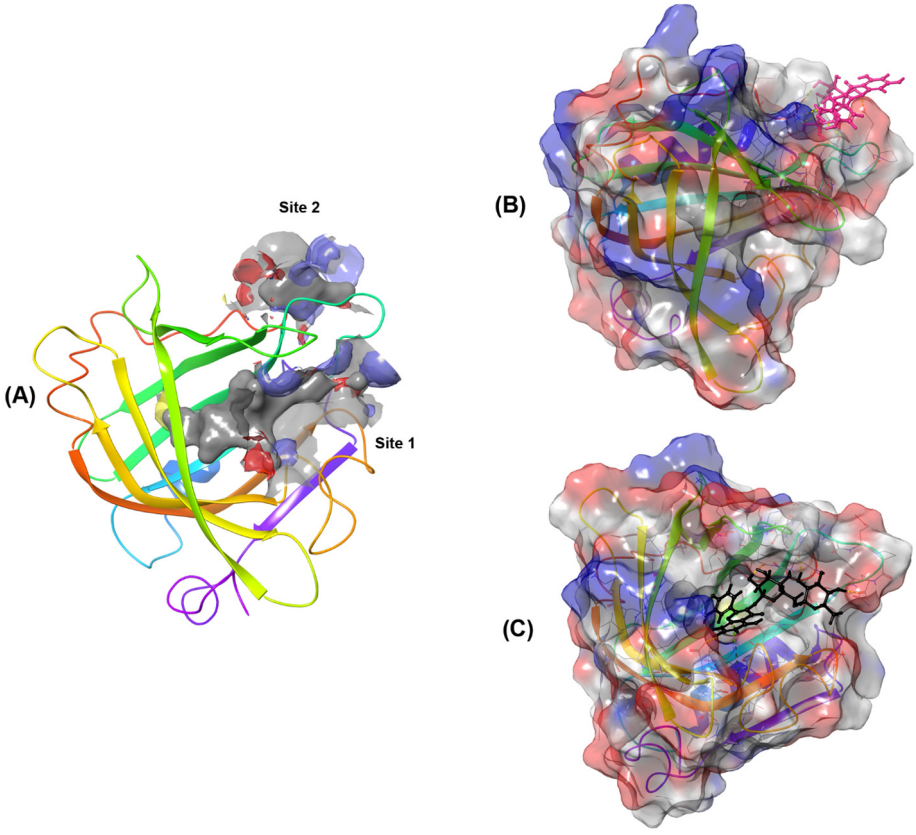

Fig. 7. Molecular docking of rutin with BLG. (A) (i) Prediction of binding site using SiteMap. Two binding sites 1 and 2 are shown, (B) Surface representation of site 2 with bound rutin, (C) Surface representation of site 1 with bound rutin.

Table 5
Interaction of rutin with BLG.

Binding sites	Hydrogen bonds	H-bond distance (Å)	Hydrophobic interactions	Other residues	Binding energy (kcal/mol)[#]	Binding affinity (M^{-1})	MM-GBSA (kcal/mol)
Site 1	Glu62, Asn88, Asn90, Asn109, Glu114, Ser116	1.77–2.74	Leu31, Pro38, Leu39, Val41, Ile56, Leu58, Ile84, Ala86, Leu87, Val92, Phe105, Met107, Ala111	Asp28, Lys60 (Pi-Pi interaction)	−9.187	5.47×10^6	−88.1516
Site 2	Leu1, Lys91[*], Glu108, Ser110, Ala111, Glu112	1.79–2.67	Ile1, Ile2, Ala111	Asn109, Gln115	−6.076	2.86×10^5	−68.0112

[*] These residues form two hydrogen bonds.
[#] Indicates binding energy in extra-precision (XP) mode.

The percent secondary structure of free BLG and BLG bound with rutin was calculated by CDNN software and values are listed in Table 4. The far-UV CD results are also suggesting that the secondary structure of BLG was found to be incursed due to rutin binding.

3.8. Molecular docking of rutin with BLG

In silico molecular docking is a well established technique used to explore the mechanism of protin-ligand interaction. Here, we used molecular docking to gain an insight into the binding mechanism of rutin with BLG protein. We used SiteMap to identify the potential binding sites on an unliganded crystal structure of BLG. It leads to the identification of two most probable binding sites, named as Site 1 and Site 2. Site 1 was located deep into the internal cavity of β-barrel, while Site 2 was identified to be located at the outskirts of β-barrel (Fig. 7). Site 1 is a primary binding site harboring a large hydrophobic cavity in which several ligands have been reported to bind [17]. In a previous study, it has been reported that BLG contains three binding sites, however, hydrophobic Site 1 remained the primary binding site [44]. Here, we used Schrodinger suite to perform molecular docking of rutin with BLG at Site 1 as well as Site 2. First we performed standard precision (SP) docking which generated multiple poses of low energies, however, we selected only the best poses with lowest energy for extra precision (XP) docking and MM-GBSA to gain insight into molecular interactions, binding affinities, binding energies and orientations of the protein-ligand interactions (Fig. 7 and Table 5).

The docking complex of rutin with BLG was stabilized by six hydrogen bonds at Site 1 and seven hydrogen bonds at Site 2. At site 1, rutin formed hydrogen bonds with Glu62, Asn88, Asn90, Asn109, Glu114 and Ser116 while at site 2, hydrogen bonds with Leu1, Lys91 (2 hydrogen bonds), Glu108, Ser110, Ala111 and Glu112. Hydrophobic interactions also played a significant role in stabilizing the complex at Site 1. Rutin formed thirteen hydrophobic interactions with Leu31, Pro38, Leu39, Val41, Ile56, Leu58, Ile84, Ala86, Leu87, Val92, Phe105, Met107 and Ala111 at Site 1 of BLG. Conversely, hydrophobic interaction played only a minor role in stabilizing rutin at Site 2 as it interacted with only three residues (Ile1, Ile2 and Ala111) shown in Fig. 8. Thus, it is clear from the molecular docking study that the interaction between rutin and BLG was driven not only by hydrogen bonding but hydrophobic interactions also played a significant role. Sahihi et al. also observed that hydrogen bonding together with hydrophobic interactions plays substantial role in the interaction of different polyphenol flavonoids with BLG [17]. In another study, the interaction between curcumin derivatives and human serum albumin was stabilized by hydrogen bonding and hydrophobic interactions [46].

Moreover, the docking score or binding energy of rutin-BLG interaction was estimated to be −9.187 kcal/mol and −6.076 kcal/mol for Site 1 in SP and XP mode, respectively. Similarly, the binding energy of rutin-BLG interaction was valued to be −6.195 kcal/mol and −5.194 for Site 2 in SP and XP mode, respectively. The binding affinity was calculated from the binding energies in XP mode and was calculated to be 5.47×10^6 M^{-1} and 2.86×10^5 M^{-1} for Site 1 and Site 2, respectively. The binding affinity of rutin with BLG has been previously reported to be of the order of 10^4 M^{-1} which is 100-folds lower that the one we observed in this study [17]. The most convincing explanation for this discrepancy is that in our study we found that rutin was bound at the inner hydrophobic cavity of β-barrel and made extensive contacts with the protein, while it was bound only superficially at the opening of the cavity in a previous study [17]. Further, we have estimated the MMPBSA (Molecular Mechanics energies combined with Poisson-

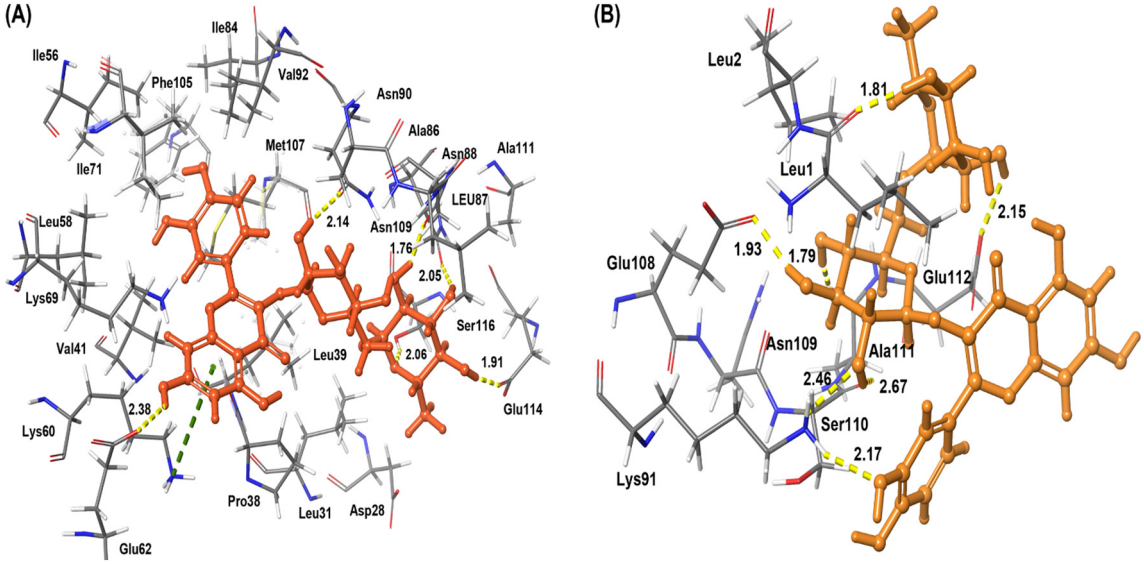

Fig. 8. Amino acid residues and the nature of interaction between rutin and BLG at site 1 (A) and (B) Amino acid residues and the nature of interaction between rutin and BLG at site 2.

Boltzmann or generalized Born and surface area continuum solvation) energies for accurately determining the strength of ligand-protein interaction. The MM/GBSA energies of rutin-BLG complex at Site 1 and Site 2 were found to be −88.1516 kcal/mol and −68.0112 kcal/mol, respectively.

3.9. MD simulation study

MD simulation was used to mimic the dynamic nature of BLG-rutin interaction under physiological conditions and to confirm the stability of BLG-rutin complex as predicted by Glide docking. The initial conformations of rutin bound at site 1 of BLG was used for MD simulation for 30 ns. Fig. 9A, shows RMSD of protein backbone after MD simulation with respect to the initial original frame. Protein backbone RMSD showed a large deviation for initial 500 ps due to stabilization of the initial protein structure. The system was stabilized after 500 ps and showed steady state dynamics. Protein backbone RMSD in the 2–15 ns was in the range of 1.0 Å to 1.6 Å as compared to that of original structure. The protein-ligand complex was stabilized only after 15 ns of simulation. The protein RMSD in the 15–30 ns was within the range of 1.2–1.4 Å, which was much lower than the prescribed 2.0 Å cutoff. Similarly, RMSD of ligand fitted on protein backbone showed drastic fluctuation during the initial phase of MD simulation. However, the ligand RMSD was stabilized during the latter part of MD simulation in the 15–30 ns range (Fig. 9A). Similar pattern was also seen in the radius of gyration of ligand (Fig. 9B). Before the start of MD simulation, radius of gyration of rutin in solution was estimated to be 5.0 Å. It showed marked decrease in the 0–10 ns MD simulation run and reached 4.4 Å level. However, after 15 ns of MD simulation it remained stabilized at 4.4 Å. Together, these results suggest that the initial fluctuation in the RMSDs of protein as well as ligand was might be due to the entry of a big ligand like rutin into the hydrophobic cavity of BLG. Once favorable interactions were formed between rutin and BLG, a stable rutin-BLG complex was demonstrated in the MD simulation.

It is also clear from MD simulation that various inter-molecular interactions such as hydrogen bonding, hydrophobic and ionic interactions as well as water bridges were formed between rutin and BLG (Fig. 9C). Moreover, Fig. 9D showed a schematic diagram of the rutin interacting with BLG. It is clear from Fig. 9C and D that hydrogen bonding and hydrophobic interaction were predominantly responsible for the formation of a stable BLG-rutin complex. We found that Glu62, Asp85 and Asn90 of BLG were involved in forming hydrogen bonds with rutin, while Leu39, Val41 and Ile84 interacted with rutin through hydrophobic interactions.

4. Conclusion

Binding, conformational and molecular docking study of rutin with BLG has been executed in the current study. All the spectroscopic results are suggesting that rutin interacted with BLG through dynamic quenching mechanism. The thermodynamic results designated that the rutin is interacting with BLG through hydrophobic interaction.

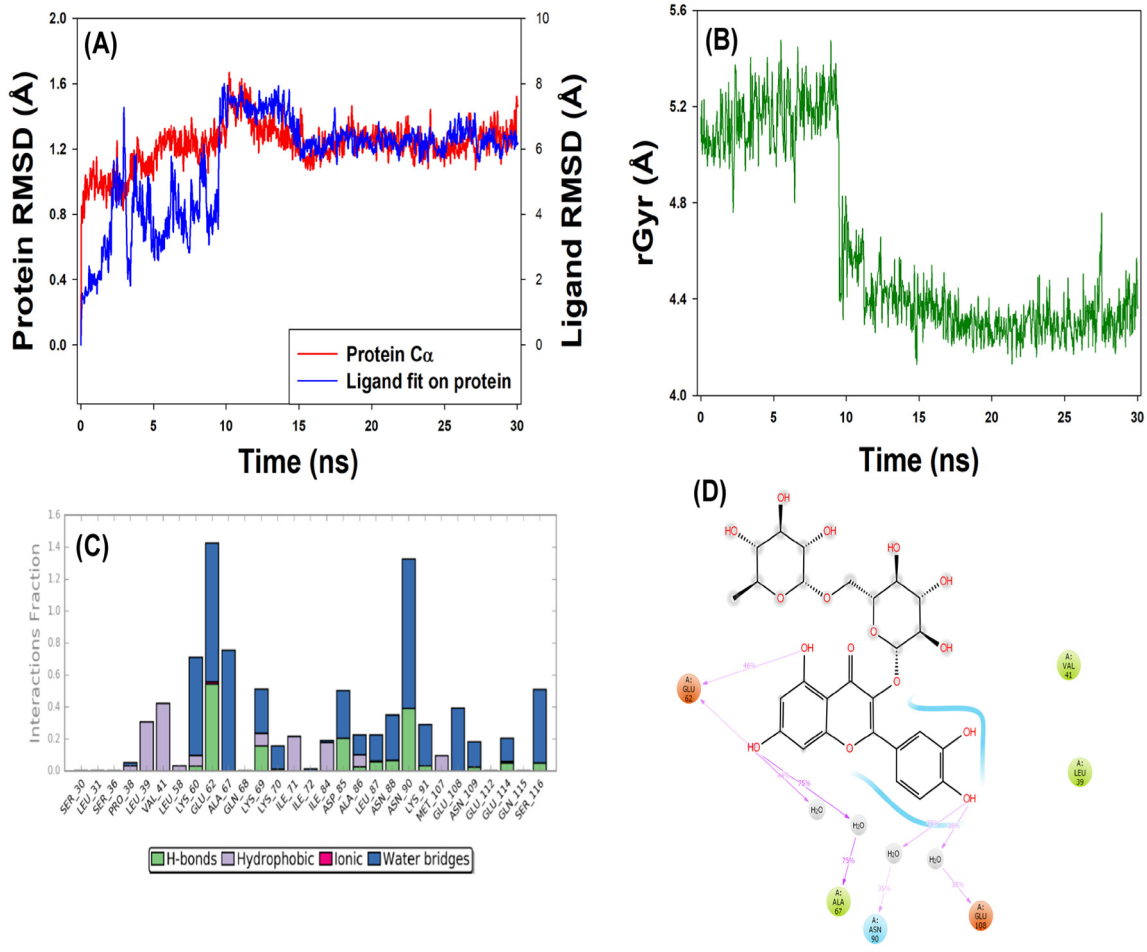

Fig. 9. MD simulation of rutin with BLG at site 1 for 30 ns. (A) RMSDs of protein and ligand, (B) Radius of gyration of ligand, (C) Bar chart showing the involvement of various interactions between rutin and BLG. The stacked bar charts are normalized over the course of the trajectory and the values over 1.0 represent the participation of amino acid residue in more than one kind of interactions with the ligand. (D) Schematic representation of amino acid residues of BLG interacting with rutin. Residues that interaction with ligand than 30% of the simulation time in the trajectory are shown.

Synchronous fluorescence results are showing that the microenvironment of BLG changed and the changes are dominantly found around the tryptophan residues. The far-UV CD results indicated that percent β-sheet structure of BLG is increased due rutin-BLG interaction. The molecular docking results are suggesting that the rutin bind to the internal cavity of BLG, which was not seen in any other reports. The molecular docking results is proposing that the rutin interacts with BLG at both site 1 and 2 through both hydrogen and hydrophobic interaction. In site 1, six amino acid residues were involved in hydrogen bonding and 13 amino acids responsible for the hydrophobic interaction. Moreover, at site 2, seven amino acids interacted through hydrogen bonding and only three amino acids bound through hydrophobic interaction. The binding affinity was found to be $5.47 \times 10^6\ M^{-1}$ and $2.86 \times 10^5\ M^{-1}$ for Site 1 and Site 2 respectively, which is >100 times compared to other molecular docking tools. MD simulation studies also suggested the formation of a stable BLG-rutin complex. The current study provides detail insights into the interaction mechanism of BLG with rutin at physiological pH, which is important for food industries, clinical medicine and life science.

Acknowledgement

The authors extend their appreciation to Deanship of Scientific Research at King Saud University for funding this work through Research Group no. RGP-1439-014.

References

[1] D.A. Devcich, I.K. Pedersen, K.J. Petrie, You eat what you are: modern health worries and the acceptance of natural and synthetic additives in functional foods, Appetite 48 (3) (2007) 333–337.
[2] M. Carocho, I.C.F.R. Ferreira, The role of phenolic compounds in the fight against cancer e a review, Anti Cancer Agents Med. Chem. 13 (2013) 1236–1258.
[3] S.L. Sankari, N.A. Babu, V. Rani, C. Priyadharsini, K.M. Masthan, Flavonoids - clinical effects and applications in dentistry: a review, J. Pharm. Bioallied Sci. 6 (Suppl. 1) (2014) S26–S29.
[4] M. Lilamand, E. Kelaiditi, S. Guyonnet, R. Antonelli Incalzi, A. Raynaud-Simon, B. Vellas, M. Cesari, Flavonoids and arterial stiffness: promising perspectives, Nutr. Metab. Cardiovasc. Dis. 24 (7) (2014) 698–704.
[5] L. Testai, Flavonoids and mitochondrial pharmacology: a new paradigm for cardioprotection, Life Sci. 135 (2015) 68–76.
[6] X. Wang, L.L. He, B. Liu, X. Wang, L. Xu, X.F. Wang, T. Sun, Decrease of the affinity of theophylline bind to serum proteins induced by flavonoids and their synergies on protein conformation, Int. J. Biol. Macromol. S0141–8130 (17) (2017) 32436.
[7] L.S. Chua, A review on plant-based rutin extraction methods and its pharmacological activities, J. Ethnopharmacol. 150 (3) (2013) 805–817.
[8] M.M. Khan, A. Ahmad, T. Ishrat, G. Khuwaja, P. Srivastawa, M.B. Khan, S.S. Raza, H. Javed, K. Vaibhav, A. Khan, F. Islam, Rutin protects the neural damage induced by transient focal ischemia in rats, Brain Res. 1292 (2009) 123–135.
[9] M.K. Araruna, S.A. Brito, M.F. Morais-Braga, K.K. Santos, T.M. Souza, T.R. Leite, J.G. Costa, H.D. Coutinho, Evaluation of antibiotic & antibiotic modifying activity of pilocarpine & rutin, Indian J. Med. Res. 135 (2012) 252–254.
[10] S. Johann, B.G. Mendes, F.C. Missau, M.A. Rezende, M.G. Pizzollati, Antifungal activity of five species of Polygala, Braz. J. Microbiol. 42 (2011) 1065–1075.
[11] A. Ganeshpurkar, A.K. Saluja, The Pharmacological potential of Rutin, Saudi Pharm. J. 25 (2) (2017) 149–164.
[12] X. Wang, Y. Liu, L.L. He, B. Liu, S.Y. Zhang, X. Ye, J.J. Jing, J.F. Zhang, M. Gao, X. Wang, Spectroscopic investigation on the food components-drug interaction: the influence of flavonoids on the affinity of nifedipine to human serum albumin, Food Chem. Toxicol. 78 (2015) 42–51.
[13] D.R. Flower, Multiple molecular recognition properties of the lipocalin protein family, J. Mol. Recognit. 8 (1995) 185–195.
[14] S. Schlehuber, A. Skerra, Lipocalins in drug discovery: from natural ligand-binding proteins to anticalins, Drug Discov. Today 10 (1) (2005) 23–33.
[15] L. Sawyer, G. Kontopidis, The core lipocalin, bovine β-lactoglobulin, Biochim. Biophys. Acta 1482 (1–2) (2000) 136–148.
[16] S. Brownlow, J.H.M. Cabral, R. Cooper, D.R. Flwoer, S.J. Yewdall, I. Polikarpov, A.C.T. North, L. Sawyer, Bovine [beta]-lactoglobulin at 1.8 Å resolution—still an enigmatic lipocalin, Structure 5 (4) (1997) 481–495.
[17] M. Sahihi, Z. Heidari-Koholi, A.K. Bordbar, The interaction of polyphenol flavonoids with β-lactoglobulin: molecular docking and molecular dynamics simulation studies, J. Macromol. Sci., Part B 51 (12) (2012) 2311–2323.
[18] M.A. Rub, J.M. Khan, N. Azum, A.M. Asiri, Influence of antidepressant clomipramine hydrochloride drug on human serum albumin: Spectroscopic study, J. Mol. Liq. 241 (2017) 91–98.
[19] J. Li, J. Li, Y. Jiao, C. Dong, Spectroscopic analysis and molecular modeling on the interaction of jatrorrhizine with human serum albumin (HSA), Spectrochim. Acta A Mol. Biomol. Spectrosc. 118 (2014) 48–54.
[20] J.R. Lakowicz, G. Weber, Quenching of fluorescence by oxygen. Probe for structural fluctuations in macromolecules, Biochemistry 12 (1973) (1973) 4161–4170.
[21] J. Loch, A. Polit, A. Gorecki, P. Bonarek, K. Kurpiewska, M. Dziedzicka-Wasylewsk, K. Lewinski, Two modes of fatty acid binding to bovine b-lactoglobulin—crystallographic and spectroscopic studies, J. Mol. Recognit. 24 (2011) 341–349.
[22] M.T. Rehman, H. Shamsi, A.U. Khan, Insight into the binding of imipenem to human serum albumin by spectroscopic and computational approaches, Mol. Pharm. 11 (2014) 1785–1797.
[23] M.T. Rehman, S. Ahmed, A.U. Khan, Interaction of meropenem with 'N' and 'B' isoforms of human serum albumin: a spectroscopic and molecular docking study, J. Biomol. Struct. Dyn. 34 (9) (2016) 1849–1864.
[24] H. Mohammadzadeh-Aghdash, J. Ezzati Nazhad Dolatabadi, P. Dehghan, V. Panahi-Azar, A. Barzegar, Multi-spectroscopic and molecular modeling studies of bovine serum albumin interaction with sodium acetate food additive, Food Chem. 228 (2017) 265–269.
[25] Q. Sun, J. He, H. Yang, S. Li, L. Zhao, H. Li, Analysis of binding properties and interaction of thiabendazole and its metabolite with humanserum albumin via multiple spectroscopic methods, Food Chem. 233 (2017) 190–196.
[26] J.D. Brennan, Using intrinsic fluorescence to investigate proteins entrapped in sol-gel derived materials, Appl. Spectrosc. 53 (1999) 106A–121A.
[27] N.A. Al-Shabib, J.M. Khan, M.S. Ali, H.A. Al-Lohedan, M.S. Khan, A.M. Al-Senaidy, F.M. Husain, M.B. Shamsi, Exploring the mode of binding between food additive "butylated hydroxytoluene (BHT)" and human serum albumin: spectroscopic as well as molecular docking study, J. Mol. Liq. 230 (2017) 557–564.
[28] A.M. Alanazi, A.S. Abdelhameed, A spectroscopic approach to investigate the molecular interactions between the newly approved irreversible ErbB blocker "Afatinib" and bovine serum albumin, PLoS One 11 (1) (2016) e0146297.
[29] J.R. Albani, J. Vogelaer, L. Bretesche, D. Kmiecik, Tryptophan 19 residue is the origin of bovine β-lactoglobulin fluorescence, J. Pharm. Biomed. Anal. 91 (2014) 144–150.
[30] Y.Y. Lou, K.L. Zhou, D.Q. Pan, J.L. Shen, J.H. Shi, Spectroscopic and molecular docking approaches for investigating conformation and bindingcharacteristics of clonazepam with bovine serum albumin (BSA), J. Photochem. Photobiol. B Biol. 167 (2017) 158–167.
[31] J.R. Lakowicz, Principles of Fluorescence Spectroscopy, Springer Science & Business Media, 2007.
[32] H. Lin, J. Lan, M. Guan, F. Sheng, H. Zhang, Spectroscopic investigation of interaction between mangiferin and bovine serum albumin, Spectrochim. Acta A Mol. Biomol. Spectrosc. 5 (2009) 936–941.
[33] R. Punith, J. Seetharamappa, Spectral characterization of the binding and conformational changes of serum albumins upon interaction with an anticancer drug, anastrozole, Spectrochim. Acta A Mol. Biomol. Spectrosc. 92 (2012) 37–41.
[34] X. Zhao, R. Liu, Z. Chi, Y. Teng, P. Qin, New insights into the behavior of bovine serum albumin adsorbed onto carbon nanotubes comprehensive spectroscopic studies, J. Phys. Chem. B 114 (2010) 5625–5631.
[35] J.R. Lakowicz, G. Weber, Quenching of fluorescence by oxygen. A probe for structural fluctuations in macromolecules, Biochemistry 12 (1973) (1973) 4161–4170.
[36] Y. Li, W. He, J. Liu, F. Sheng, Z. Hu, X. Chen, Binding of the bioactive component jatrorrhizine to human serum albumin, Biochim. Biophys. Acta 1722 (2005) 15–21.
[37] P.D. Ross, S. Subramanian, Thermodynamics of protein association reactions forces contributing to stability, Biochemistry 20 (1981) 3096–3102.
[38] J.Q. Lu, F. Jin, T.Q. Sun, X.W. Zhou, Multi-spectroscopic study on interaction of bovine serum albumin with lomefloxacin–copper(II) complex, Int. J. Biol. Macromol. 40 (2007) 299–306.
[39] H. Zhang, X. Huang, P. Mei, K. Li, C. Yan, Studies on the interaction of tricyclazole with b-cyclodextrin and human serum albumin by spectroscopy, J. Fluoresc. 16 (2006) 287–294.
[40] A. Sulkowska, Interaction of drugs with bovine and human serum albumin, J. Mol. Struct. 614 (2002) 227–232.
[41] M.D. Meti, S.T. Nandibewoor, S.D. Joshi, U.A. More, S. Chimatadar, Binding interaction and conformational changes of human serum albumin with ranitidine studied by spectroscopic and time-resolved fluorescence methods, J. Iran. Chem. Soc. 13 (2016) 1325–1338.
[42] N.A. Al-Shabib, J.M. Khan, M.A. Alsenaidy, A.M. Alsenaidy, M.S. Khan, F.M. Husain, M.R. Khan, M. Naseem, P. Sen, P. Alam, R.H. Khan, Unveiling the stimulatory effects of tartrazine on human and bovine serum albuminfibrillogenesis: Spectroscopic and microscopic study, Spectrochim. Acta A Mol. Biomol. Spectrosc. 191 (2018) 116–124.
[43] M.A. Rub, A.M. Asiri, J.M. Khan, R.H. Khan, Kabir-ud-Din, Interaction of gelatin with promethazine hydrochloride: Conductimetry, tensiometry and circular dichroism studies, J. Mol. Struct. 1050 (2013) 35–42.
[44] M.A. Rub, A.M. Asiri, J.M. Khan, F. Khan, R.H. Khan, A study of interaction between antidepressant drug nortriptyline hydrochloride with gelatin, J. Taiwan Inst. Chem. Eng. 45 (2014) 2068–2074.
[45] L. Liang, H.A. Tajmir-Riahi, M. Subirade, Interaction of beta-lactoglobulin with resveratrol and its biological implications, Biomacromolecules 9 (1) (2008) 50–56.
[46] A.K. Bordbar, K. Mohammadi, A. Divsalar, A.A. Saboury, Circular dichroism and fluorescence spectroscopic study on the interaction of bisdemethoxycurcumin and diacetylbisdemethoxycurcumin with human serum albumin, Can. J. Chem. 88 (2010) 155.